Progress In Electromagnetics Research C, Vol. 172, 223–230, 2026 PIER C

(Received 26 June 2026, Accepted 25 July 2026, Scheduled 9 August 2026)

Capacity Improvement in Indoor VLC-NOMA Networks

Abdullah H. Chilmeran* and Safwan H. Younus

College of Electronics Engineering, Ninevah University, Mosul, Iraq

ABSTRACT: Visible Light Communication (VLC) combined with Non-Orthogonal Multiple Access (NOMA) is a promising technology for meeting the high-capacity demands of future 6G indoor networks. Most existing VLC-NOMA user pairing schemes rely solely on the direct-link channel gain for user ordering and ignore wall reflections that introduce spatially nonuniform interference, thereby degrading successive interference cancellation (SIC) performance. To overcome these limitations, a user ranking based on the user's effective signal-to-interference-plus-noise ratio (SINR) from both direct and indirect links is proposed, and users are paired into independent pairs with balanced SINR separation through a SINR-based user pairing framework. The proposed framework reduces interference accumulation by isolating users into independent NOMA pairs, thereby improving scalability and throughput. The results of MATLAB simulation demonstrate that the proposed scheme achieves a throughput of 710 Mbps for eight users, which is 274% higher than the 190 Mbps achieved by conventional NOMA. The proposed framework achieves 320 Mbps under imperfect SIC conditions, whereas conventional NOMA achieves 74 Mbps, demonstrating the robustness of the proposed framework under practical receiver impairments.

1. INTRODUCTION

Visible Light Communication (VLC) is a promising technology for high-speed indoor wireless communications based on light-emitting diodes (LEDs). VLC offers high bandwidth, energy efficiency, and security, but suffers from noise, interference, and signal blockage. These challenges can be mitigated by integrating VLC with Non-Orthogonal Multiple Access (NOMA), which multiplexes users in the power domain over the same resources and improves the spectral efficiency and capacity [1–3]. Parallel data transmission has been demonstrated to significantly enhance the throughput of indoor VLC systems. Consequently, VLC-NOMA further improves spectrum utilization and network capacity in dense user scenarios [4], and VLC-NOMA networks are considered promising for satisfying the increasing demand for ultra-high data rates and massive device connectivity required by future 6G indoor networks [5]. Efficient power allocation and user pairing are essential for improving the NOMA throughput [6]. Most VLC-NOMA pairing schemes consider only line-of-sight (LOS) gains while neglecting non-line-of-sight (NLOS) reflections, leading to suboptimal pairing and decoding performance. This paper investigates a downlink VLC-NOMA system, aiming to maximize capacity under realistic LOS and NLOS propagation. An interference-aware SINR-based pairing strategy is proposed to mitigate NLOS interference, improve the successive interference cancellation (SIC) performance, and enhance scalability. Practical VLC-NOMA systems experience imperfect SIC due to estimation errors, decoding, and hardware errors, resulting in residual interference and reduced throughput. Therefore, evaluating pairing robustness under imperfect SIC is essential for practical indoor VLC deployment. The proposed framework was analyzed in terms of sum rate, user reliability, and spectral efficiency. The simulation results show that the proposed SINR-based balanced user-pairing framework clearly outperforms the conventional VLC-NOMA. In particular, it supports a data rate of 710 Mbps with 8 users, which is 274% higher than the traditional NOMA. Moreover, the proposed framework is robust in practice in an indoor VLC environment with imperfect SIC condition, as it provides a throughput of 320 Mbps while the conventional NOMA achieves 74 Mbps.

The main contributions of this study are summarized as follows:

- Proposing an SINR-based user pairing scheme for VLC networks, which accounts for both LOS and NLOS components to mitigate multiple access interference.
- Developing an SINR-aware pairing framework to maximize system throughput while maintaining SIC feasibility.
- Simulations demonstrate that the proposed VLC-NOMA pairing scheme significantly improves system throughput compared with conventional NOMA systems.
- Evaluating the robustness of the proposed SINR-based pairing framework under imperfect SIC conditions and its impact on the system throughput.

The remainder of this paper is organized as follows. Section 2 reviews the related work. Section 3 describes the system and channel models. Section 4 details the proposed NOMA and user pairing mathematical framework. Section 5 presents the simulation results and performance discussions. Finally, Section 6 concludes the paper.

* Corresponding author: Abdullah Hasan Chilmeran (abdullah.ali.msc@stu.uoninevah.edu.iq).

2. RELATED WORKS

Early research on VLC-NOMA primarily focused on improving spectral efficiency through efficient power allocation. Among the first to consider NOMA in VLC downlink networks were Marshoud et al. [7], who proposed the Gain Ratio Power Allocation (GRPA) power allocation strategy and demonstrated significant gains over static allocation. Building on these early developments, Mohsan et al. [8] reviewed NOMA-based VLC systems and argued that spectral-efficiency gains require effective interference management rather than power allocation alone, a claim later confirmed empirically by Liu et al. [9], who compared NOMA and OMA in downlink VLC and showed that NOMA gains depend on user-pairing selection for a given indoor layout. This dependence pushed subsequent work toward joint optimization of user pairing and power allocation rather than treating power allocation in isolation. Obeed et al. [10] and Maraqa et al. [11] jointly optimized user pairing with resource and power allocation to improve network performance and user rates, while Zhang et al. [12] extended this line with an improved particle swarm optimization-based scheme that further enhanced the sum-rate across diverse interference scenarios through adaptive inertia weighting and elite opposition-based learning. In the same direction, Ibrahim et al. [13] confirmed the centrality of pairing strategy for MIMO-NOMA VLC systems, proposing two pairing algorithms with consistent sum-rate gains over ungrouped transmission, and this line of research remains active. Recently, [14] proposed an enhanced gain-difference power allocation scheme that exploits residual power after allocating prior users in MIMO-VLC-NOMA, and [15] jointly optimized power allocation with access-point placement for drone-assisted NOMA-VLC, confirming that pairing and allocation-aware design continues to extend beyond fixed indoor topologies. Despite this progress, Sadat et al. [16] identified a persistent gap: few studies jointly address the trade-off among sum-rate, fairness, Quality of Service (QoS), and SIC reliability, particularly under imperfect SIC. This concern is reinforced by Li et al. [17], who proposed a secure user-pairing and power-allocation strategy satisfying minimum-rate constraints per user, illustrating that pairing decisions increasingly need to balance several, sometimes competing, objectives rather than sum-rate alone. Al Hammadi et al. [18] approached the problem from yet another angle, jointly optimizing power allocation and LED transmission-angle tuning via deep Q-learning to maximize sum-rate and energy efficiency, showing that user ordering and angular configuration jointly shape achievable performance. A limitation common to [7, 9–15] is that user ordering and pairing depend almost exclusively on the DC channel gain, implicitly assuming an LOS-dominated channel in which channel gain reliably indicates received SINR. This assumption makes the analysis easier, but may restrict the potential capacity achievable in realistic propagation settings. Arfaoui et al. [19] demonstrated that experienced interference should be considered in resource allocation in addition to channel gain. This interference-aware philosophy has recently been extended to the grouping decision itself: Tu et al. [20] proposed a channel-quality indicator that embeds cross-LED interference directly into the user-grouping rule for multi-LED VLC-NOMA, showing that grouping based on channel gain alone becomes unreliable as interference strengthens. A similar pairing-under-uncertainty principle has also been explored outside VLC, where [21] proposed a channel-state-aware user-pairing scheme for NOMA-enabled vehicular networks. In indoor VLC systems, such interference can originate from both neighboring transmitters and diffuse reflections under combined LOS and NLOS propagation. Diffuse reflections from room surfaces create spatially nonuniform interference that can reduce a nominally strong user's effective SINR below that of a weaker user, making the channel-gain-based ordering unreliable and reducing overall system throughput. This is the central motivation of the present work. Although [12–15, 17] improved capacity-aware pairing and power allocation, most existing studies do not adopt a composite LOS and NLOS SINR as the pairing metric, nor consider intra-pair SINR gaps to guarantee SIC feasibility as user loads increase. The proposed framework addresses this gap directly, targeting two objectives simultaneously: increasing aggregate throughput and preserving SIC reliability under realistic LOS and NLOS conditions for all pairs.

3. SYSTEM MODEL

3.1. Room Configuration and LED Placement

We consider a typical indoor downlink VLC scenario within a rectangular room with dimensions ($6 \times 6 \times 3\,\mathrm{m}^3$). Four LED luminaires wear mounted on the ceiling in a symmetric (2×2) grid arrangement, providing both uniform illumination (≥ 400 lux, in compliance with ISO 8995-1 indoor lighting standards) and simultaneous optical data transmission to multiple users located at the receiver plane (height $h_r = 0.85\,\mathrm{m}$, representing desk level), as shown in Figure 1.

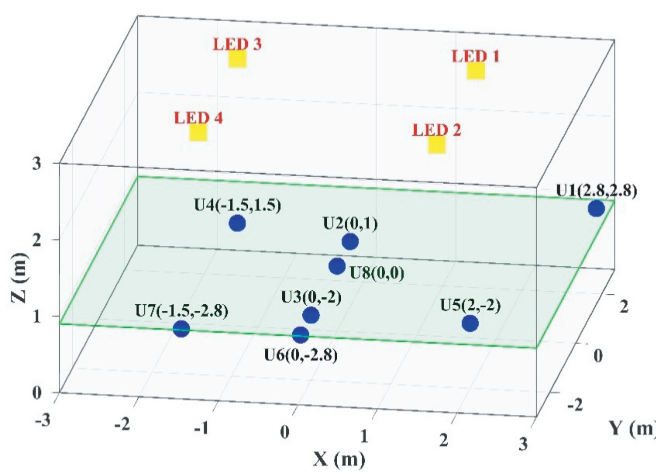

FIGURE 1. Indoor VLC system.

3.2. Optical Channel Model: LOS and NLOS Components

The optical channel in indoor VLC environments consists of two principal components: a line-of-sight (LOS) component, which carries the dominant portion of optical energy, and a non-line-of-sight (NLOS) component, which arises from first-order

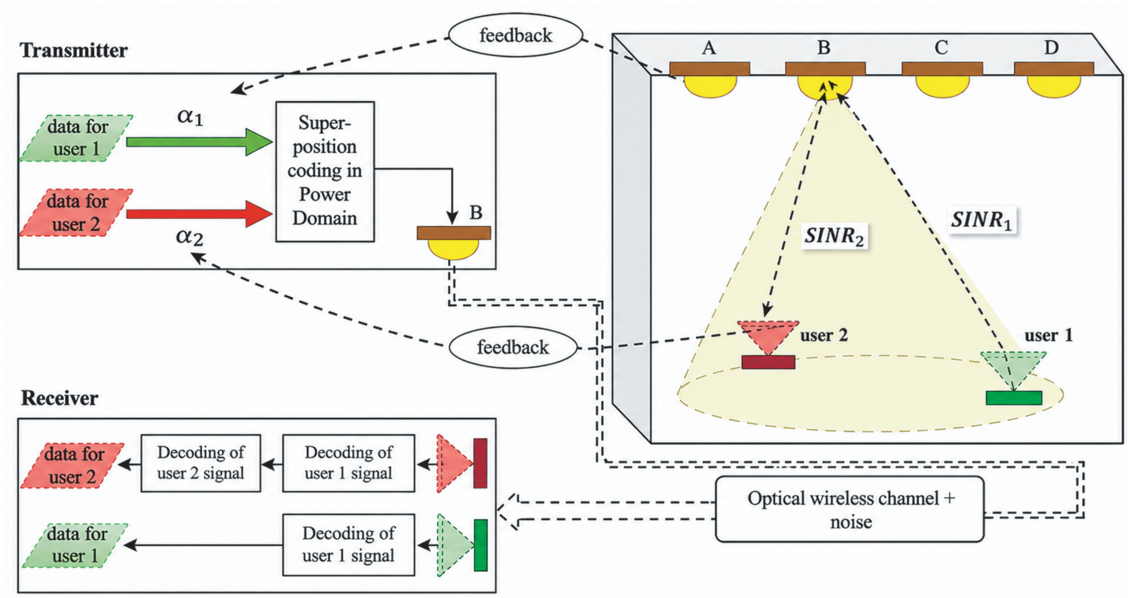

FIGURE 2. Block diagram of implementation of NOMA-based VLC system.

diffuse reflections off wall surfaces. The total DC channel gain between the l-th LED and the k-th user is therefore expressed as:

$$H_{l,k} = H_{l,k}^{LOS} + H_{l,k}^{NLOS} \tag{1}$$

The LOS channel DC gain follows a well-established Lambertian radiation model. For a clear, unobstructed optical path between the l-th LED and the k-th user, it is given by [22]:

$$H_{LOS,k} = \begin{cases} \frac{(m+1)\cdot A_{det}}{2\pi\cdot d_k^2}\cos^m(\phi_k)T_s(\psi_k)g(\psi_k)\cos(\psi_k), & 0\le\psi_k\le\Psi_c \\ 0, & \psi_k > \Psi_c \end{cases} \tag{2}$$

where $g(\psi_k)$, ϕ_k, and ψ_k denote the gains of an optical concentrator, the angle of irradiance of the LED (AP), and the angle of incidence of the k-th use's receiver, respectively; T_s is a constant denoting the optical filter gain; d_k is the distance between the AP and the k-th user; and A_{det} is the physical area of the photodetector (PD) receiver. The order of Lambertian emission is denoted by m and given by:

$$m = \frac{-\ln(2)}{\ln(\cos\Phi_{1/2})} \tag{3}$$

where $\Phi_{1/2}$ is the semi-angle of the LED. In addition, the optical concentrator gain $g(\psi_k)$ is defined as [23]:

$$g(\psi) = \begin{cases} \frac{n^2}{\sin^2\psi_c}, & 0\le\psi\le\Psi_c \\ 0, & \psi > \Psi_c \end{cases} \tag{4}$$

where n is the refractive index constant, and Ψ_c is the field-of-view angle at the user's PD receiver. The NLOS component results from optical energy that undergoes diffuse reflection from the room surfaces (walls) before reaching the receiver. To include the reflected component, the first-order NLOS gain was computed by considering contributions of the four room walls. The surfaces of the room are divided by $\mathbb{R}$ reflecting elements with an area dA. The NLOS channel gain for the k-th user can be generally expressed as [24]:

$$H_{NLOS,k} = \sum_{i=1}^{l}\sum_{j=1}^{\mathbb{R}} \frac{(m+1)\cdot A_{\text{det}}\cdot dA}{2\pi^2\cdot d_{1,w}^2\cdot d_{2,wk}^2}\cos^m(\phi_{1,w}) \rho_w\cos(\alpha_w)\cos(\beta_{wk})\ldots T_s(\psi_{kw})\,g(\psi_{kw}) \cos(\psi_{kw})\,dA_w \tag{5}$$

where ρ_w is the reflection coefficient of walls w; A_w is the wall surface element; $d_{1,w}$ is the distance from the LED to the reflecting point; $d_{2,wk}$ is the distance from the reflecting point to the k-th user; α_w is the angle of irradiance on the wall; and β_{wk} is the angle from the wall toward the receiver. The first-order reflected component was numerically evaluated by discretizing each wall into sufficiently small reflective elements and summing the contributions of all reflected paths.

4. NOMA FRAMEWORK AND USER PAIRING STRATEGY

4.1. Power-Domain NOMA Transmission

A key feature of NOMA is that multiple users can share the same time and frequency resources by allocating different power levels to their respective signals. Therefore, the transmitted signal is formed as a power-domain superposition of individual user signals [8], as illustrated in Figure 2. In the proposed VLC-PD-NOMA system, four LEDs simultaneously transmit a superimposed optical signal to K users $K \in \{2,4,6,8\}$ over the same optical bandwidth. The composite transmit signal is expressed as a weighted superposition of the individual user signals [25] as follows:

$$x(t) = \sum_{k=1}^{K}\sqrt{a_k\cdot P_{LED}}\,s_k(t) \tag{6}$$

where s_k is the normalized modulated symbol for the k-th user with $E[|s_k|^2] = 1$; P_{LED} is the total transmitted optical power per LED; and a_k is the power allocation coefficient for user k, satisfying [26]:

$$\sum_{k=1}^{k} a_k = 1, \quad 0 < a_k < 1 \quad \forall k \tag{7}$$

Accurate channel state information (CSI) is essential for power allocation and user ordering in the proposed system. The access point (AP) obtains the composite channel DC gain H_k of each user, including both the LOS and NLOS components. The CSI is estimated at the photodetector (PD) and fed back to the AP, which uses it to compute the users' SINRs, perform NOMA ordering, and assign power allocation coefficients.

Remark 1 (CSI and NLOS): In indoor VLC environments, NLOS reflections introduce spatially varying signal and interference levels. Therefore, the composite channel gain H_k alone may not accurately reflect the reception quality of a user, motivating the use of SINR as the primary user-ordering metric.

4.2. Received Signal and SINR with SIC

The received photocurrent at user k is [25]:

$$y_k(t) = R \cdot H_k \cdot x(t) + n_k(t) \tag{8}$$

where R (A/W) is the PD responsivity, and $nk \sim \mathcal{N}(0, \sigma^2)$ is the additive Gaussian white noise (AWGN) with variance $\sigma^2 = N_0 B$, where N_0 is the noise power spectral density, and B is the modulation bandwidth.

In conventional NOMA, users are ordered according to their channel gain H_k. However, NLOS reflections can make H_k an unreliable indicator of user performance because users with higher channel gains may experience lower effective SINRs due to increased interference. Therefore, the user ordering in this study was based on the instantaneous received SINR. The initial (pre-ordering) SINR at user k is expressed as:

$$SINR_k^{init} = \frac{R^2 \cdot H_k^2 \cdot P_{LED}}{ISI + \sigma^2} \tag{9}$$

where ISI represents the localized interference power predominantly caused by the (NLOS) reflections ($ISI = R^2 H_{nlos}^2 P_{LED}$).

Using the CSI reported by all users, the AP computes (9) for each user and sorts them in ascending order of $SINR^{init}$:

$$SINR_1^{init} \leq SINR_2^{init} \leq \ldots \leq SINR_K^{init} \tag{10}$$

This SINR-based ordering (10) replaces the conventional channel-gain-based ordering. The index $k = 1$ now denotes the user with the weakest effective SINR (highest interference impact), which is assigned the highest power coefficient, and $k = K$ denotes the user with the strongest effective SINR, assigned the lowest power coefficient: $a_1 \geq a_2 \geq \ldots \geq a_K$. Figure 3 shows the throughput comparison between both ordering methods for 8 users.

Remark 2 (SINR-based ordering in LOS and NLOS channels): In LOS-dominated channels, ordering by the channel

Algorithm 1 NOMA SINR-based ordering

1. **INPUT**: room dimensions, LED positions, user position, system parameters
2. Set: θ, *A*, ψ, *n*, *P_total*, *B*, *R*, Room dimensions (*x*, *y*, *z*)
3. Compute: *m* and *g* (ψ)

------ LOS channel gain ------

4. **for** each TX *i* = 1 ... *k*:
5. IF ψ ≤ FOV:
6. Compute: $H_{LOS,k}$

------ NLOS channel gain ------

7. **for** each wall in {West, East, North, South}:
8. Compute: $H_{NLOS,k}$
9. **end**
10. **end**
11. Compute: noise σ^2
12. Compute: $SINR^{intial}$ for CSI
13. Assign Power Allocation (a_k) for each user based on $SINR^{intial}$
14. Compute: $SINR_k$, BER_k, $Rate_k$ and Throughput

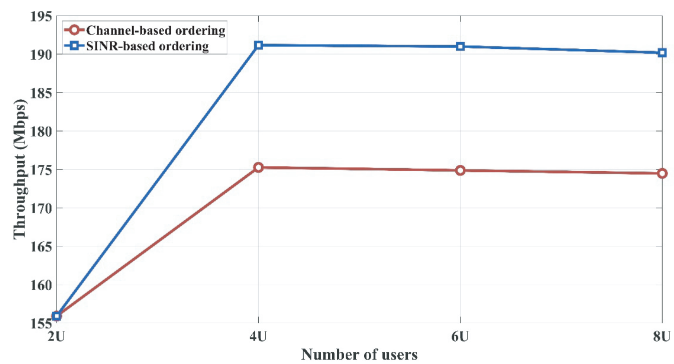

FIGURE 3. Throughput comparison between channel and SINR-based ordering for 8 users.

gain H_k is generally equivalent to ordering by the SINR. However, under LOS and NLOS propagation, a user with higher H_k may experience a lower SINR owing to increased reflected interference, leading to inefficient power allocation. The SINR-based ordering in (10) avoids this issue by considering the actual interference experienced by each user.

4.3. SIC Detection and Post-SIC SINR

After SINR-based ordering is established, SIC is applied to each receiver. User k decodes and cancels the users' signals $j < k$ (those with a weaker SINR and allocated higher power) before decoding its own signal. The signals of users $j > k$ remain as residual interference. The post-SIC SINR at user k is expressed as:

$$SINR_k = \frac{R^2 \cdot H_k^2 \cdot a_k \cdot P_{LED}}{\left(R^2 \cdot H_k^2 \cdot \sum_{j=k+1}^{K} a_j \cdot P_{LED} + ISI + \sigma^2\right)} \tag{11}$$

The denominator of (11) contains only the signals of users $j > k$ (stronger SINR users, not yet cancelled) and the noise variance σ^2. For the strongest user ($k = K$), no interference remains after perfect SIC:

$$SINR_K = \frac{R^2 \cdot H_K^2 \cdot a_K \cdot P_{LED}}{ISI + \sigma_K^2} \tag{12}$$

Practical VLC systems often suffer from imperfect SIC due to hardware limitations, decoding errors, and imperfect channel estimation. This results in residual interference from the weaker users that were not completely cancelled. To model this, let β represent the residual interference error fraction, where $0 \leq \beta \leq 1$. The generalized post-SIC SINR at user k under imperfect SIC can be formulated as:

$$SINR_k = \frac{R^2 \cdot H_k^2 \cdot a_k \cdot P_{LED}}{\left(R^2 \cdot H_k^2 \cdot \sum_{j=k+1}^{K} a_j \cdot P_{LED} + \beta \cdot R^2 \cdot H_k^2 \cdot \sum_{j=1}^{k-1} a_j \cdot P_{LED} + ISI + \sigma^2\right)} \tag{13}$$

When $\beta = 0$, the system achieves perfect SIC, simplified to Equation (11). In our simulations, $\beta > 0$ is used to evaluate system robustness with practical receiver impairments. The achievable data rate and system sum-rate are [26]:

$$C_k = B \cdot \log_2 (1 + SINR_k) \tag{14}$$

$$C_{sum} = \sum_{k=1}^{K} C_k \tag{15}$$

4.4. Balanced User Pairing Strategy

After SINR-based ordering, users are grouped into NOMA pairs using a balanced pairing strategy that ensures a sufficient intra-pair SINR gap for effective NOMA operation. Unlike extreme pairing, which matches the weakest and strongest users, the proposed approach distributes the SINR gap more evenly by symmetrically pairing users in the ordered SINR list. Specifically, for K ordered users, the i-th user is paired with the $(i + K/2)$-th user as follows:

$$\Omega = \left\{ \left(U_i, U_{i+K/2}\right) \mid i = 1, 2, \dots, K/2 \right\} \tag{16}$$

This pairing rule ensures that each weak user (lower half of the SINR-ordered list) is paired with a user from the upper half, thereby maintaining a consistent SINR gap in each pair. Table 1 shows the resulting pairs for $K \in \{2, 4, 6, 8\}$.

Pairing logic: For $K = 4$: U_1 pairs with U_3 (gap = 2), and U_2 pairs with U_4 (gap = 2). For $K = 6$: U_1 pairs with U_4, U_2 with U_5, and U_3 with U_6 (uniform gap = 3 in all pairs) and so on.

TABLE 1. Balanced user pairing (Ω) for $K = 2, 4, 6$, and 8 users.

K	Pair	Pair 1	Pair 2	Pair 3	Pair 4
$K = 2$	1	(U_1, U_2)	—	—	—
$K = 4$	2	(U_1, U_3)	(U_2, U_4)	—	—
$K = 6$	3	(U_1, U_4)	(U_2, U_5)	(U_3, U_6)	—
$K = 8$	4	(U_1, U_5)	(U_2, U_6)	(U_3, U_7)	(U_4, U_8)

Algorithm 2 NOMA SINR-Balanced ordering

INPUT: Total number of users K, Pre-ordering $SINR^{intial}$ array from Algorithm 1, Total transmit power P_{LED}

Sort users based on collected CSI feedback as in Eq. (10)
Initialize: Pairing list Ω
---- Balanced User Pairing Formation ----
for $i = 1$ *to* $K/2$:
  Identify weak user: $U_{weak} = U_i$
  Identify strong user: $U_{strong} = U_{i+K/2}$
  Form pair: $P_i = (U_{weak}, U_{strong})$
  Append P_i to Ω
end
---- Intra-Pair Decoding ----
for each pair P_i in Ω:
  Assign power coefficients α_{weak} and α_{strong} satisfying $\alpha_{weak} > \alpha_{strong}$
  At U_{strong} Receiver:
  Execute successive interference canceler to decode and subtract U_{weak} signal
  Compute post-SIC $SINR_{strong}$
  At U_{weak} Receiver:
  Decode signal directly (treating U_{strong} signal as residual noise)
  Compute $SINR_{weak}$
end
Compute: Individual data rates C_k for all users
Compute: System Throughput $C_{sum} = sum\ C_k$

This uniform-gap design ensures that every pair has a similar intra-pair SINR difference, avoiding the scenario in which one pair benefits disproportionately from a large SINR gap while another pair suffers from a negligible one, which is a known drawback of extreme (first-with-last) pairing in multi-user systems

5. SIMULATION RESULTS AND DISCUSSION

Extensive MATLAB simulations were conducted to comprehensively evaluate the performance of the proposed SINR-based balanced user pairing strategy. The simulated indoor VLC environment consisted of a rectangular room measuring $6 \times 6 \times 3\,\text{m}^3$. The main parameters used in these simulations are summarized in Table 2. The primary objective is to compare the proposed user pairing framework with a conventional channel-gain-based NOMA system across varying network loads ($K \in \{2, 4, 6, 8\}$).

The maximum number of multiplexed users considered in this study is limited to eight owing to practical hardware constraints and the increased complexity and error propagation of SIC with larger user counts. To isolate the effects of multiple-access interference and user pairing, user locations remain fixed as the number of users increases. Furthermore, a deterministic ray-tracing channel model is adopted to accurately characterize the LOS and first-order reflected optical propagation in the considered indoor VLC environment. In addition, a Fixed Power Allocation (FPA) scheme is adopted, with power coefficients determined by the number of active users. The performance analysis focuses on edge user U_1 at (2.8, 2.8), representing the worst-case propagation condition.

TABLE 2. Simulation parameters.

Description	Symbol	Value
Transmitters Locations	l	$(1.5, 1.5), (1.5, -1.5), (-1.5, 1.5), (-1.5, -1.5)$
Transmitted power	P_{LED}	72 W
Transmitter semi-angle	$\Phi_{1/2}$	70°
Modulation bandwidth	B	20 MHz
PD detection area	A_{det}	1 cm^2
PD Locations	k	$(2.8, 2.8), (0, 1), (0, -2), (-1.5, 1.5), (2, -2), (0, -2.8), (-1.5, -2.8), (0, 0)$
Responsivity	R	0.53 A/W
Optical filter gain	T_s	1
FOV of PD	ψ_c	90°
reflection coefficient of walls	ρ_w	0.8
refractive index of a lens at a PD	n	1.5
interference error fraction	β	0.1

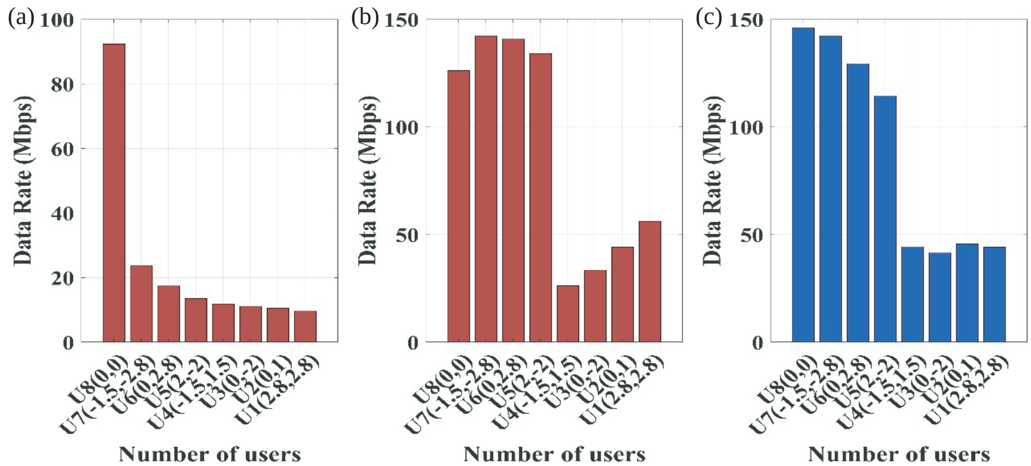

FIGURE 4. Perfect SIC per-user data rate for (a) conventional NOMA, (b) near/far pairing, and (c) balanced user pairing.

5.1. Per-User Data Rate Analysis

The individual data rates of all eight users ($K = 8$) were analyzed to evaluate system fairness and robustness under both perfect and imperfect SIC. Under perfect SIC, as shown in Figure 4, conventional NOMA exhibits an uneven rate distribution, where the strongest user U_8 achieves approximately 92 Mbps, whereas the remaining users achieve only 10–24 Mbps, resulting in a total sum-rate of approximately 190 Mbps. In contrast, the proposed balanced pairing scheme achieves a more uniform rate distribution of 42–147 Mbps and increases the sum-rate to approximately 710 Mbps. For further comparison, the near-far pairing strategy was also evaluated. The near-far pairing strategy achieves system throughput comparable to the proposed method under the fixed user deployment, and it exhibits a pronounced imbalance in individual user data rates, as illustrated in Figure 4(b). Users with stronger channel conditions obtain significantly higher data rates, whereas weaker users experience considerably lower rates. Such performance disparity indicates reduced user fairness and may increase the sensitivity of the SIC process to residual interference, particularly for users with intermediate channel conditions. In contrast, the proposed balanced pairing framework provides a more uniform distribution of user performance while maintaining high achievable throughput. Figure 5 shows the imperfect SIC, and conventional NOMA suffers a significant performance loss, reducing user rates to 7.8 to 10 Mbps and the total sum-rate to 74 Mbps. Conversely, the proposed scheme maintains user rates between 35 and 46 Mbps, achieving a sum-rate of approximately 320 Mbps, which is more than four times that of conventional NOMA. These results demonstrate that the proposed pairing framework improves both fairness and capacity while maintaining robustness against imperfections in the SIC.

5.2. System Throughput Performance

Figure 6 compares the total system throughput of the conventional NOMA and the proposed balanced pairing scheme for different network loads $K = 2, 4, 6$, and 8 under perfect and imperfect SIC conditions. Under perfect SIC, both schemes achieve approximately 155 Mbps at $K = 2$, but conventional NOMA saturates at approximately 190 Mbps for $K \geq 4$ owing

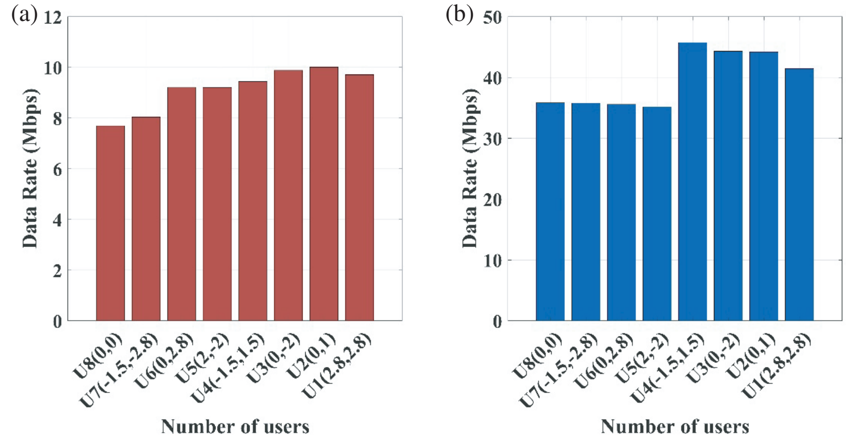

FIGURE 5. Imperfect SIC per-user data rate for (a) conventional NOMA and (b) balanced user pairing.

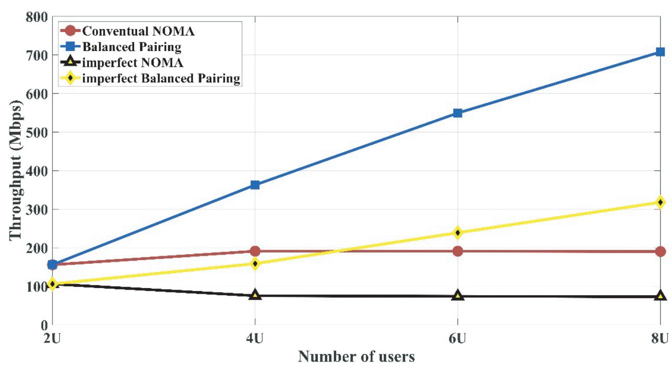

FIGURE 6. Perfect and imperfect SIC throughput vs. number of users on conventional NOMA and balanced user pairing.

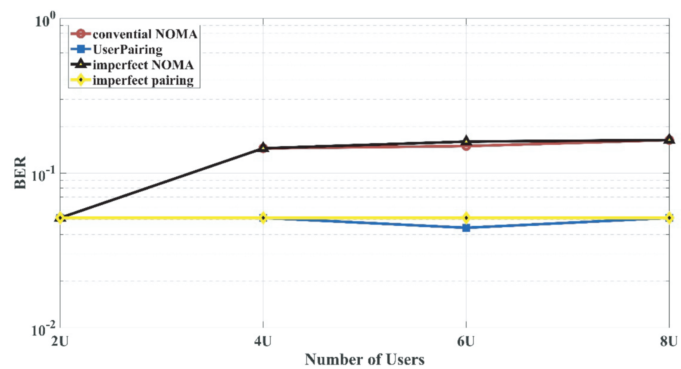

FIGURE 7. Perfect and imperfect SIC BER performance for conventional NOMA and balanced user pairing.

to increased interference. In contrast, the proposed scheme enables near-linear throughput scaling by forming isolated SINR-based pairs, reaching 710 Mbps at $K = 8$, representing a 273% improvement. Under imperfect SIC, both schemes started at approximately 106 Mbps for $K = 2$. As the number of users increases, the conventional NOMA decreases to 74 Mbps at $K = 8$ because of the accumulated residual interference, whereas the proposed scheme maintains robustness by limiting the interference within each pair and achieves 320 Mbps, providing a 332% gain. These results confirm that the proposed pairing framework improves both the capacity and robustness of dense indoor VLC-NOMA networks.

5.3. Reliability and Bit Error Rate (BER) Performance

The system reliability is evaluated using the BER of edge user U_1, as shown in Figure 7. For $K = 2$, all the schemes achieve a BER of approximately 5×10^{-2} owing to limited interference. However, as the number of users increases, conventional NOMA suffers severe BER degradation, reaching approximately 1.5×10^{-1} under both perfect and imperfect SIC. This degradation results from single-group multiplexing and channel-gain-based ordering, which increases NLOS-induced interference and disrupts SIC decoding. In contrast, the proposed SINR-based pairing scheme maintains a stable BER of approximately 5×10^{-2} for $K = 4, 6, 8$, even with imperfect SIC. By forming isolated pairs with controlled SINR gaps, the proposed framework limits interference to the paired user, preserves SIC feasibility, and improves edge-user reliability in dense VLC-NOMA networks.

6. CONCLUSION

In this study, the downlink capacity of an indoor VLC-NOMA system was investigated under realistic LOS and NLOS propagation conditions. To overcome the limitations of conventional channel-gain-based ordering, a balanced SINR-based user pairing scheme was proposed, in which users are grouped into independent two-user NOMA pairs according to their composite LOS and NLOS SINRs. By limiting interference within each pair, the proposed framework improves SIC performance and enables near-linear sum-rate scaling with increasing user load. The simulation results confirmed the effectiveness of the proposed scheme. Under perfect SIC, the system sum-rate increased from 155 Mbps at $K = 2$ to 710 Mbps at $K = 8$, while conventional NOMA saturated at approximately 190 Mbps beyond $K = 4$, achieving a 273% improvement under full load. In addition, the proposed framework distributes capacity gains more evenly among users rather than concentrating them on a single dominant user. Under imperfect SIC, the proposed scheme achieved 320 Mbps at $K = 8$ compared to 74 Mbps for conventional NOMA, corresponding to a 332% throughput gain. It also maintained a stable edge-user data rate of approximately 41 Mbps and a BER of 5×10^{-2} across all network loads. One limitation of this study is the use of fixed power allocation coefficients, which do not exploit the potential gains of joint power allocation and user pairing optimization. In addition, the user locations were fixed to isolate pairing effects from spatial variations. Future work will focus on (i) integrating SINR-based pairing with dynamic power allocation, (ii) extending the framework to multi-cell VLC-NOMA networks with inter-cell interference, and (iii) validating the proposed scheme on a practical VLC testbed under realistic propagation and SIC error conditions.

REFERENCES

[1] Ding, Z., X. Lei, G. K. Karagiannidis, R. Schober, J. Yuan, and V. K. Bhargava, "A survey on non-orthogonal multiple access for 5G networks: Research challenges and future trends," *IEEE Journal on Selected Areas in Communications*, Vol. 35, No. 10, 2181–2195, 2017.

[2] Lin, B., X. Tang, Y. Li, M. Zhang, Z. Ghassemlooy, Y. Wei, Y. Wu, and H. Li, "Block interleaved frequency division multiple access for visible light communications," in *2017 16th International Conference on Optical Communications and Networks (ICOCN)*, 1–3, Wuzhen, China, 2017.

[3] Jian, Y.-H., C.-C. Wang, C.-W. Chow, W. H. Gunawan, T.-C. Wei, Y. Liu, and C.-H. Yeh, "Optical beam steerable orthogonal frequency division multiplexing (OFDM) non-orthogonal multiple access (NOMA) visible light communication using spatial-light modulator based reconfigurable intelligent surface," *IEEE Photonics Journal*, Vol. 15, No. 4, 1–8, 2023.

[4] Younus, S. H., A. A. Al-Hameed, A. T. Hussein, M. T. Alresheedi, and J. M. H. Elmirghani, "Parallel data transmission in indoor visible light communication systems," *IEEE Access*, Vol. 7, 1126–1138, 2018.

[5] Chen, S., Y.-C. Liang, S. Sun, S. Kang, W. Cheng, and M. Peng, "Vision, requirements, and technology trend of 6G: How to tackle the challenges of system coverage, capacity, user data-rate and movement speed," *IEEE Wireless Communications*, Vol. 27, No. 2, 218–228, 2020.

[6] El-Banna, H. H. and N. M. Shafik, "Comparative study for channel pairing in NOMA OFDM-CDMA system," *Mansoura Engineering Journal*, Vol. 50, No. 6, 7, 2025.

[7] Marshoud, H., V. M. Kapinas, G. K. Karagiannidis, and S. Muhaidat, "Non-orthogonal multiple access for visible light communications," *IEEE Photonics Technology Letters*, Vol. 28, No. 1, 51–54, 2016.

[8] Mohsan, S. A. H., M. Sadiq, Y. Li, A. V. Shvetsov, S. V. Shvetsova, and M. Shafiq, "NOMA-based VLC systems: A comprehensive review," *Sensors*, Vol. 23, No. 6, 2960, 2023.

[9] Liu, Z., F. Yang, J. Song, and Z. Han, "Multiple access for downlink multi-user VLC system: NOMA or OMA user pairing?" *IEEE Wireless Communications Letters*, Vol. 12, No. 11, 1916–1920, 2023.

[10] Obeed, M., H. Dahrouj, A. M. Salhab, S. A. Zummo, and M.-S. Alouini, "User pairing, link selection, and power allocation for cooperative NOMA hybrid VLC/RF systems," *IEEE Transactions on Wireless Communications*, Vol. 20, No. 3, 1785–1800, 2021.

[11] Maraqa, O., U. F. Siddiqi, S. Al-Ahmadi, and S. M. Sait, "On the achievable max-min user rates in multi-carrier centralized NOMA-VLC networks," *Sensors*, Vol. 21, No. 11, 3705, 2021.

[12] Zhang, H., J. Li, J. Tang, H. Hu, Y. Cao, Y. Wang, Y. Liu, T. Tang, Q. Li, and L. Shi, "Power allocation for sum-rate maximization in VLC-NOMA systems with improved particle swarm optimization," *Electronics*, Vol. 15, No. 7, 1378, 2026.

[13] Ibrahim, H. S., M. Abaza, A. Mansour, and A. Alfalou, "Performance analysis of power allocation and user-pairing techniques for MIMO-NOMA in VLC systems," *Photonics*, Vol. 11, No. 3, 206, 2024.

[14] Zhong, X., P. Miao, and X. Wang, "Enhanced gain difference power allocation for NOMA-based visible light communications," *Electronics*, Vol. 13, No. 4, 776, 2024.

[15] Liang, J., M. Pang, and X. Ke, "Research on resource allocation algorithm for non-orthogonal multiple access visible light communication," *Photonics*, Vol. 11, No. 11, 1042, 2024.

[16] Sadat, H., M. Abaza, A. Mansour, and A. Alfalou, "A survey of NOMA for VLC systems: Research challenges and future trends," *Sensors*, Vol. 22, No. 4, 1395, 2022.

[17] Li, Y., Y. Chen, and X. Ji, "Secure user pairing and power allocation for downlink non-orthogonal multiple access against external eavesdropping," *Entropy*, Vol. 26, No. 1, 64, 2024.

[18] Al Hammadi, A., L. Bariah, S. Muhaidat, M. Al-Qutayri, P. C. Sofotasios, and M. Debbah, "Deep Q-learning-based resource allocation in NOMA visible light communications," *IEEE Open Journal of the Communications Society*, Vol. 3, 2284–2297, 2022.

[19] Arfaoui, M. A., A. Ghrayeb, C. Assi, and M. Qaraqe, "CoMP-assisted NOMA and cooperative NOMA in indoor VLC cellular systems," *IEEE Transactions on Communications*, Vol. 70, No. 9, 6020–6034, 2022.

[20] Tu, Y., C. Li, and C. V. Pham, "Interference-aware user grouping and power allocation for overlapping multi-LED ADO-OFDM NOMA VLC networks," *Photonics*, Vol. 13, No. 3, 241, 2026.

[21] Balaraman, A., S. Shioda, Y. Kim, Y. Kim, and T. Kim, "Efficient user pairing and resource optimization for NOMA-OMA switching enabled dynamic urban vehicular networks," *Electronics*, Vol. 13, No. 23, 4834, 2024.

[22] Marshoud, H., P. C. Sofotasios, S. Muhaidat, G. K. Karagiannidis, and B. S. Sharif, "On the performance of visible light communication systems with non-orthogonal multiple access," *IEEE Transactions on Wireless Communications*, Vol. 16, No. 10, 6350–6364, 2017.

[23] Tao, S., H. Yu, Q. Li, and Y. Tang, "Performance analysis of gain ratio power allocation strategies for non-orthogonal multiple access in indoor visible light communication networks," *EURASIP Journal on Wireless Communications and Networking*, Vol. 2018, No. 1, 154, 2018.

[24] Ghassemlooy, Z., W. Popoola, and S. Rajbhandari, *Optical Wireless Communications: System and Channel Modelling with MATLAB®*, CRC Press, 2019.

[25] Ngene, C. E., P. Thakur, and G. Singh, "Perfect and imperfect successive interference cancellation for channel decoding in downlink visible light non-orthogonal multiple access network," *Optik*, Vol. 287, 171129, 2023.

[26] Aldababsa, M., M. Toka, S. Gökçeli, G. K. Kurt, and O. Kucur, "A tutorial on nonorthogonal multiple access for 5G and beyond," *Wireless Communications and Mobile Computing*, Vol. 2018, No. 1, 9713450, 2018.